A NUMERICAL SIMULATION OF TRANSITION BOILING HEAT TRANSFER

Shigeo MARUYAMA, Masahiro SHOJI, and Satoshi SHIMIZU

Department of Mechanical Engineering, Faculty of Engineering, The University of Tokyo
7-3-1 Hongo, Bunkyo-ku, Tokyo 113, Japan

ABSTRACT

Time dependent dry-patterns of the macro-layer and heat transfer from a boiling surface for high heat flux nucleate boiling, critical heat flux condition, and transition boiling are numerically simulated. Assuming an initial spatial pattern of vapor stems with random positions and random sizes, growth of each vapor stem as well as the decay of the thickness of macro-layer are calculated based on a simple one-dimensional heat conduction model. Employing the experimental variation of initial thickness of the macro-layer with wall superheat, the predicted boiling curve agrees well with the experimental one. In addition to the dry patterns of macro-layer, time-progress of wall void fraction, equivalent thickness of macro-layer, and heat flux are predicted. Simulated results are compared with the spatially averaged model and the time averaged one of macro-layer.

INTRODUCTION

The evaporation of macro-layer under each coalesced bubble is considered to be a key mechanism to understand the high heat flux nucleate boiling, critical heat flux, and transition boiling. There are several models of the macro-layer which describe the boiling heat transfer in these regimes. One of them is the model view by Katto et al. [1,2] which firstly suggested that the evaporation of the macro-layer under the coalesced bubble is the primary mechanism of heat removal from the surface. The time sequence of the evaporation of liquid layer during the bubble hovering period was considered. Assuming that higher the nucleate heat flux, thinner the thickness of macro-layer at the time of liquid supply, the critical heat flux occurs when the supplied liquid is completely dry out before the next liquid supply. Hence, in the transition boiling regime, complete dry out phase with very poor heat transfer appears in each period of bubble hovering. Recent model of Pan et al.[3] described the detailed process of macro-layer formation and evaporation based on the similar idea.

Another model recently proposed by Dhir and Liaw[4] described apparently different scenario of critical heat flux and transition boiling. They explained the boiling curve through the measured time-averaged wall void fraction[5]. They made a model of dry pattern with regularly distributed constant diameter vapor stems. Based on their heat conduction considerations, they argued that the total length of vapor-liquid interface (periphery of vapor stems) determined the effectiveness of evaporation. The measured wall void fraction monotonically increased with wall superheat. With their model of regularly placed vapor stems, the periphery becomes maximum when the wall void fraction is $\pi/4$, which corresponds to the maximum of heat flux or critical heat flux condition.

Both models seem to nicely explain the physical mechanism, though they have a considerable discrepancies. For better understandings of the real phenomena, we calculated the time consequences of the two-dimensional dry pattern with a simple model. As a result, it was demonstrated that the former view [1-3] can be recognized as the spatial averaged model and the latter[4] the time averaged model.

METHOD OF NUMERICAL SIMULATION

In order to simulate the change of dry pattern during the period of bubble hovering, the initial dry pattern at the time of liquid supply (t = 0) is assumed as follows. The thickness of the macro-layer δ_0 and initial wall void fraction α_0 were employed from the experimental correlations of Shoji et al.[6]. Circular vapor stems with random radii are located at random positions of 14 mm x 14 mm square surface filled with the macro-layer of thickness δ_0 until the assumed initial void fraction is satisfied. For the random radius of vapor stem we forced an upper limit of r_{max}.

To consider the time evolution of the macro-layer, we calculated the decay of the thickness and the growth of the each vapor stem with a simple heat conduction model. For the macro-layer thickness, the vertical one-dimensional heat conduction through the liquid layer is calculated from the linear temperature distribution between the constant wall temperature and the saturated temperature. The thickness of the layer $\delta(t)$ is estimated to be

$$-\frac{d\delta}{dt} = \frac{1}{\rho_l H_{fg}} \frac{\lambda \Delta T}{\delta}, \tag{1}$$

where λ is heat conductivity of liquid, ρ_l is density of liquid, H_{fg} is latent heat of evaporation, and ΔT is wall superheat. Eq. (1) can be solved independent of the dry pattern as

$$\delta(t) = \sqrt{\delta_0^2 - 2\frac{\lambda \Delta T}{\rho_l H_{fg}} t}. \tag{2}$$

On the other hand, estimation of the growth rate dr_s/dt of the vapor stem radius is not straightforward. Assuming the angle θ of the liquid layer to the wall be constant as shown in Fig. 1, we can calculate the evaporation from the area of r to r+dr by the vertical one-dimensional heat conduction. Then, the integral to r gives the total amount of evaporation from the sloped area. Assuming that the remained liquid keeps the same angled shape, the radius r_s must increase as

$$\frac{dr_s}{dt} = \frac{1}{\rho_l H_{fg}} \frac{\lambda \Delta T}{\delta} \frac{1}{\tan\theta} \left[1 + \log\left(\frac{\delta}{\delta_m}\right)\right], \tag{3}$$

where δ_m is employed to avoid the infinite heat flux right at the liquid-vapor interface in this simple model. Using the upper

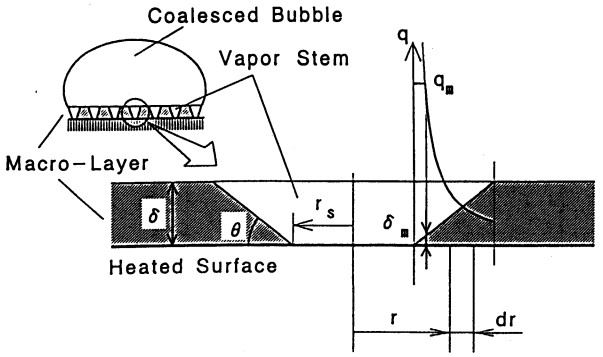

Fig. 1 Model of heat conduction and evaporation near the liquid–vapor interface. Note that this shape of vapor stem is assumed only when calculating the growth rate of vapor stems. Cylindrical vapor stems are assumed for other calculations.

limit of the heat transfer by evaporation which is estimated through a consideration of molecular motion, q_m = 7.86 ΔT (MW/m²) for saturated boiling of water at atmospheric pressure[7], δ_m is expressed as $q_m = \lambda\Delta T/\delta_m$.

Since the actual shape of the vapor stem has not experimentally determined, the simple estimation in eq. (3) is rather crude and may need to be subjected to a refinement. Because the evaporation of liquid is dominant right at the contact circle on the wall, the shape of vapor stems is more likely to be cylindrical(θ = 90° in Fig. 1). We used eq. (3) and the shape of Fig. 1 only for the simplicity of the estimation of growth rate. Since the growth rate expressed as eq. (3) is not a function of r_s, it can be easily extended to an arbitrary shaped vapor stem. Employing eq. (3) is equivalent to an assumption that liquid–vapor interface grows at a constant rate proportional to the wall superheat and reciprocally proportional to the thickness of the macro-layer. Then, we consider the parameter tanθ as the ratio of decay of thickness to the growth of vapor layer rather than the physical contact angle.

CHANGE OF DRY PATTERN, MACRO-LAYER THICKNESS, AND HEAT FLUX

Fig. 2 shows an example of the numerical simulations related to the critical heat flux condition of saturated pool boiling of water at atmospheric pressure. Fig. 2(a) is the initially assumed dry pattern at t = 0. White circular parts represent the vapor stems. For the wall superheat ΔT = 23 K, initial thickness δ_0 = 33 μm and initial void fraction α_0 = 0.1 is assumed (see next section for details). The circular region is 10 mm diameter control area, and vapor stems with random sizes but smaller than r_{max} = 0.4 mm (see next section) are distributed at random positions. The parameter θ is determined to be 6° as discussed later. Fig. 2(b)–(d) are results of decay of thickness and growth of radii. Initially isolated vapor stems begin to merge together and finally islands of liquid area are formed {Fig. 2(d)}.

Fig. 3 is the corresponding time chart of thickness δ and void fraction α. The equivalent thickness W = δ(1−α) expresses the amount of liquid left on the surface. Then, the instantaneous heat flux q is expressed as

$$\begin{aligned} q &= \rho_l H_{fg}\left(-\frac{dW}{dt}\right) = \rho_l H_{fg}\left(-\frac{d\{\delta(1-\alpha)\}}{dt}\right) \\ &= \rho_l H_{fg}(1-\alpha)\left(-\frac{d\delta}{dt}\right) + \rho_l H_{fg}\delta\left(\frac{d\alpha}{dt}\right) \\ &= q_\delta + q_\alpha, \end{aligned} \tag{4}$$

where q_δ and q_α are heat flux consumed by the decay of macro-layer thickness and growth of vapor stems, respectively. These forms of heat flux are plotted in Fig. 3. Note that the rugged feature of the curves is due to the finite resolution of the numerical calculation of void fraction. An interesting

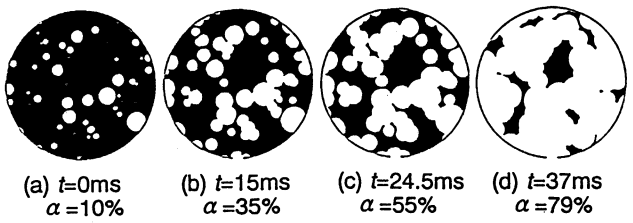

Fig. 2 Simulated dry patterns for CHF condition of ΔT = 23K, $\bar{q}$ = 1.4 MW/m².

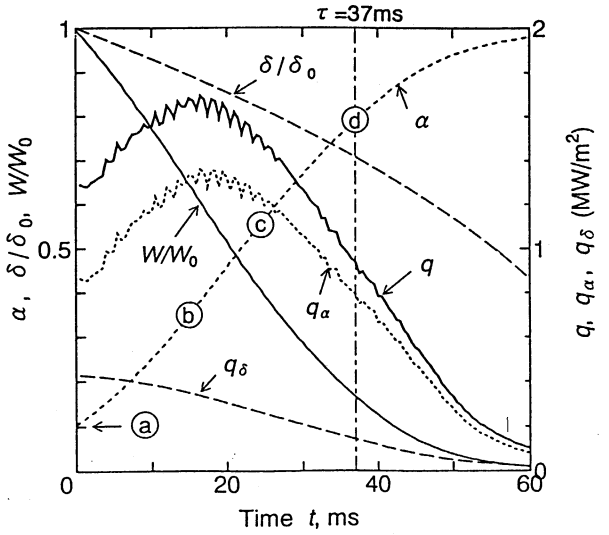

Fig. 3 Change of void fraction α, thickness of macro-layer δ, and instantaneous heat flux q for CHF condition.

feature is that the heat flux q has the maximum at about 17 ms due to the maximum of q_α. This time roughly corresponds to the dry pattern with the maximum periphery of vapor stems (Fig. 2), which occurs when α is 0.4 to 0.5. In this case, macro-layer completely dried out at 71 ms as void fraction reaches 1.0. However, when ΔT is larger or δ_0 is smaller, the decay of thickness is dominant and the dry-out time tends to be $\delta_0^2\rho_l H_{fg}/(2\lambda\Delta T)$ from eq. (2). The liquid supply will occur at the period of hovering bubble τ, and the averaged heat flux $\bar{q}$ will be the integration of q from t = 0 to t = τ.

BOILING CURVES

Assumption of initial thickness of the macro-layer, initial void fraction, and bubble hovering interval are necessary to simulate the change of heat transfer with wall superheat. Shoji et al. [6] have measured the initial thickness of macro-layer on 10 mm copper surface under the steady state transition boiling and they have obtained an experimental correlation for the heat flux. To obtain a correlation of the thickness to wall superheat, we need to assume the nucleate heat flux for transition boiling regime. Regarding that the upper envelop of the fluctuating boiling curve by Shoji et al.[8] (Fig. 5) expresses the nucleate heat flux for transition boiling regime, the initial thickness was calculated as shown in Fig. 4.

For the initial void fraction α_0, Gaertner and Westwater[9] gave the constant value of 0.11 for the nucleate boiling. Shoji et al.[6] had reported almost the same value. For the transition boiling regime, to our knowledge, no measurement has been done. So, we assumed a constant value of 0.1 regardless of the wall superheat.

The hovering interval τ of bubble was accurately measured by Shoji et al.[6]. It was almost constant in nucleate boiling to critical heat flux at about 37 ms, and gradually increased in the transition boiling regime. Ignoring this relatively small increase, we assumed it to be constant at 37 ms

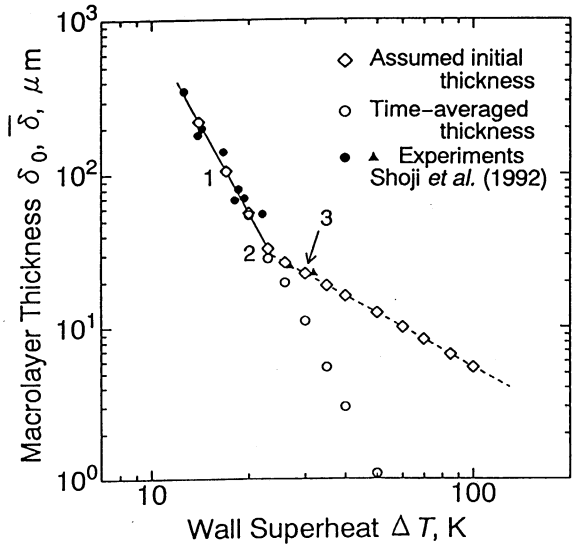

Fig. 4 Assumed initial thickness of macro-layer.

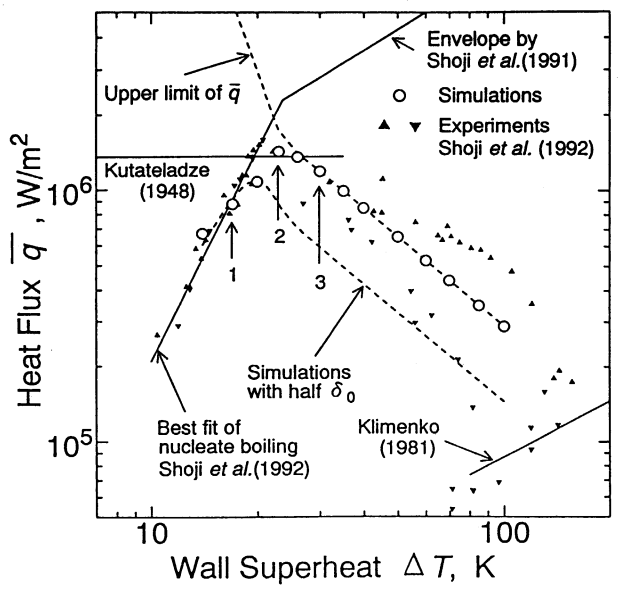

Fig. 5 Simulated boiling curves.

regardless of the wall superheat.

The boiling curve shown in Fig. 5 was obtained after numerically optimizing the two parameters to be θ = 6° and r_{max} = 0.4 mm. Satisfactory good agreement of the simulated averaged heat flux and the experimental data by Shoji et al.[6] is noticed. Here, the experimental data agreed fairly well with the classical correlation of Kutateladze[10] for critical heat flux and with the film boiling heat flux correlation of Klimenko[11]. The simulated result marked as 2 turned out to be the critical heat flux condition which is regarded as CHF in Figs. 2, 3, 6, and 7. According to the assumptions of δ_0, α_0, and τ, the upper limit of average heat flux $\bar{q}_{max}$ is calculated as $\bar{q}_{max} = \rho_l H_{fg} \delta_0 (1-\alpha_0)/\tau$ as shown in Fig. 5. In the transition boiling regime, the simulated averaged heat flux almost fell on this line, which means the complete dry out before the bubble hovering period τ.

To consider the effect of the contact angle on the boiling curve, the initial thickness δ_0 was reduced to the half of the experimental correlation shown in Fig. 4, as expected for larger contact angle[12]. Then, the resultant averaged heat flux shown with a dotted line is much lower in transition boiling regime and almost the same in the nucleate boiling regime.

SPATIALLY AVERAGED AND TIME AVERAGED MODELS

Spatially Averaged Model

Fig. 6 demonstrates the periodic change of heat flux and equivalent thickness for (1) nucleate boiling, (2) critical heat flux condition and (3) transition boiling. The random number set determining the initial radii and positions of vapor stems are altered for each 3 period. The effect of this randomness is found to be negligible. Fig. 6 well reproduces the view of Katto et al.[1,2]. In their model the change of void fraction was not considered and was assumed to be the constant value determined experimentally by Gaertner and Westwater[9]. However, if we regard the equivalent thickness $W = \delta(1-\alpha)$ as their macro-layer thickness, these can be compared each other. The use of the equivalent thickness corresponds to taking the spatial average of the simulated dry patterns.

In the nucleate boiling regime, initially thick macro-layer prevails until the next liquid supply. The difference from their model is the condition of the critical heat flux. The critical heat flux condition in present simulation occurs when small amount of liquid is still on the wall at the end of each period. Because the instantaneous heat flux has its maximum and decreases from its maximum value with time, the heat flux considerably decreases at later stages of the period when the macro-layer has completely dried out.

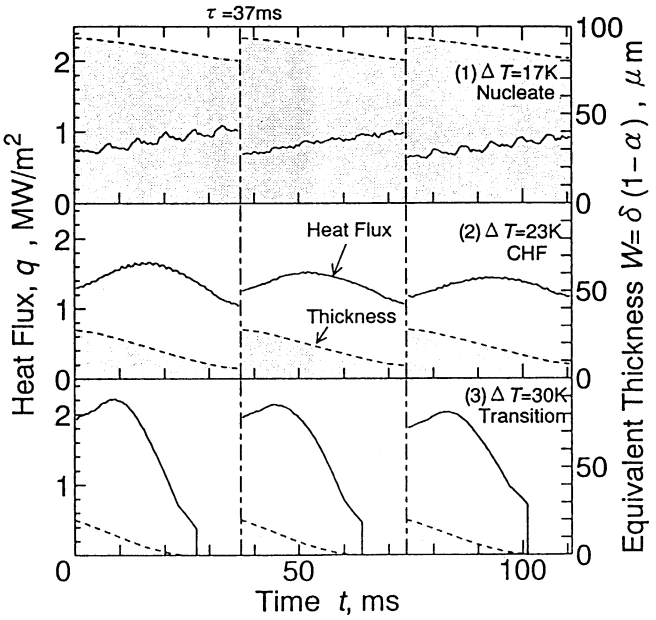

Fig. 6 Periodic change of heat flux and equivalent thickness of macro-layer for (1) nucleate boiling, (2) CHF, (3) transition boiling. These conditions correspond to marks 1, 2 and 3 in the boiling curve (Fig. 5).

An indirect measurement of the instantaneous heat flux was performed more than 20 years ago by Katto et al.[2]. They had measured the instantaneous volume V of each coalesced bubble from the high speed motion pictures as shown in Fig. 7. If we assume that all heat flux from the wall is used to evaporate the liquid, the change of bubble volume is calculated as

$$\frac{dV}{dt} = \frac{q}{\rho_v H_{fg}}. \qquad (5)$$

In Fig. 7 calculated volume change of the bubble from the simulated heat flux is also plotted. Katto et al.[2] defined their origin of time when the bubble actually departed from the wall. However, according to the motion pictures, the liquid-supply from the side of the bubble was initiated about 8 ms before their time-origin. We assume that our initial condition of calculation is 8 ms before their time-origin for the compari-

son in Fig. 7. The drastic change of the tendency of bubble growth from near CHF condition to the transition boiling is well reproduced by the simulation.

Time Averaged Model

The time averaged model of Dhir and Liaw[4] can also be reproduced from the simulated results. Time averaged wall void fraction are plotted in Fig. 8 for the comparison with experimental data. In the nucleate boiling regime, the growth of the vapor stems is slow and the averaged void fraction is not far from the initially assumed value α_0. Then, near the critical heat flux condition, it rapidly increases to near 0.5 and tends to 1.0 in transition boiling regime. The simulated void fraction is in good agreement with experimental results by Shoji et al.[6] and Liaw and Dhir[5]. Dhir and Liaw[4] demonstrated the effect of contact angle on the boiling curve through the difference of these experimental wall void fraction. The simulated data with half initial thickness related to the larger contact angle qualitatively agreed with their results. In principle, the time averaging of present simulation will reduce to their model.

NOMENCLATURE

H_{fg} = latent heat of evaporation, J/kg
q = instantaneous heat flux, W/m^2
q_α = $\rho_l H_{fg} \delta (d\alpha/dt)$ = heat flux consumed by the increase of void fraction, W/m^2
q_δ = $\rho_l H_{fg} (1-\alpha)(-d\delta/dt)$ = heat flux consumed by the decay of the macro-layer thickness, W/m^2
$\overline{q}$ = time averaged heat flux, W/m^2
$\overline{q}_{max}$ = Upper limit of the averaged heat flux, W/m^2
r = radial coordinate from the center of the vapor stem, m
r_s = radius of vapor stem, m
r_{max} = maximum radius of the initial vapor stem, m
t = time, s
V = volume of coalescence bubble, m^3
W = amount of liquid $W = (1-\alpha)\delta$, m

Greek symbols
α = wall void fraction
$\overline{\alpha}$ = time averaged wall void fraction
δ = thickness of macro-layer, m
ΔT = wall superheat, K
ϕ = contact angle, deg.
λ = heat conductivity, W/(mK)
θ = angle parameter of the heat conduction model, deg.
ρ_l = density of liquid, kg/m^3
ρ_v = density of vapor, kg/m^3
τ = hovering period of bubble, s

Subscripts
0 = initial condition
m = maximum limit of evaporation

REFERENCES

1. Katto, Y. and Yokoya, S., Int. J. Heat Mass Transfer, vol. 11, pp. 993–1002, 1968.
2. Katto, Y., Yokoya, S. and Yasunaka, M., Proc. 4th Int. Heat Transfer Conf., Paris, vol. 5, p. B3.2, 1970.
3. Pan, C., Hwang, J. Y. and Lin, T. L., Int. J. Heat Mass Transfer, vol. 32, pp. 1337–1349, 1989.
4. Dhir, V. K. and Liaw, S. P., Trans. ASME, J. Heat Transfer, vol. 111, pp. 739–746, 1989.
5. Liaw, S. P. and Dhir, V. K., Trans. ASME, J. Heat Transfer, vol. 111, pp. 731–738, 1989.
6. Shoji, M., Huang, Z. L., Tanaka, T. and Yokoya, S., Proc. 29th National Heat Transfer Symp., Osaka, pp. 301–302, 1992.
7. Shoji, M., Proc. 2nd Typical Workshop, JSHT, pp. 66–70, 1990.

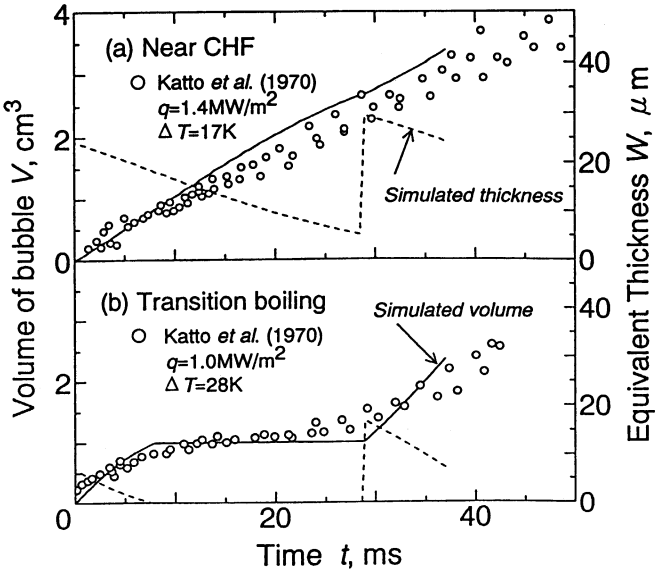

Fig. 7 Growth of bubbe volume for (a) nucleate boiling near CHF compared with simulated CHF condition of ΔT=23K, $\overline{q}$=1.4MW/m^2 (marked 2 in Fig. 5) and (b) transition boiling compared with the simulation of ΔT=35K, $\overline{q}$=0.99MW/m^2.

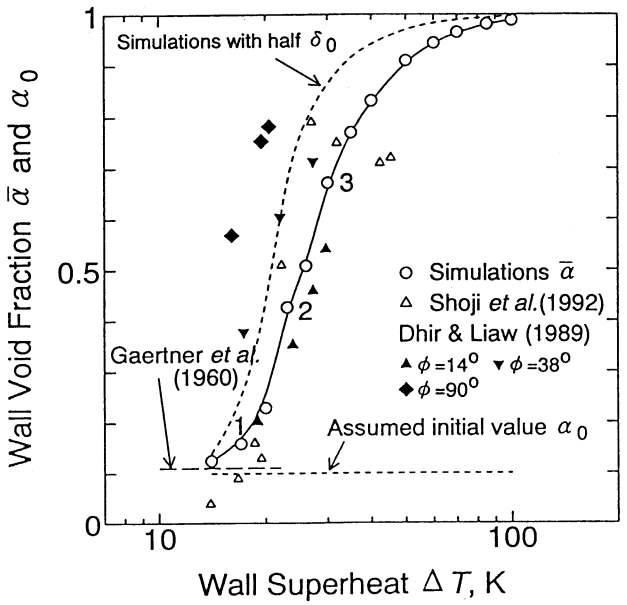

Fig. 8 Time averaged wall void fraction.

8. Shoji, M., Witte, L. C., Yokoya, S., Kawakami, M. and Kuroki, H., 3rd ASME-JSME Therm. Engng. Joint Conf. 2, pp. 333–338, 1991.
9. Gaertner, R. F. and Westwater, J. W., Chem. Eng. Prog. Symp. Ser. 56–30, pp. 39–48, 1960.
10. Kutateladze, S. S., Kotlotubostoenie, vol. 3, p. 10, 1948.
11. Klimenko, V. V., Int. J. Heat Mass Transfer, vol. 24, pp. 69–79, 1981.
12. Shoji, M., Kuroki, H and Tokumasu, T., Proc. 29th National Heat Transfer Symp., Osaka, pp. 432–433, 1992.